Ecological Applications, 17(5), 2007, pp. 1543–1554

PREDICITNG EXTINCTION RISK IN SPITE OF PREDATOR–PREY OSCILLATIONS

John L. Sabo[1] and Leah R. Gerber

Faculty of Ecology, Evolution and Environmental Science, School of Life Sciences, Arizona State University, P.O. Box 874501, Tempe, Arizona 85287-4501 USA

Abstract. Most population viability analyses (PVA) assume that the effects of species interactions are *subsumed* by population-level parameters. We examine how robust five commonly used PVA models are to violations of this assumption. We develop a stochastic, stage-structured predator–prey model and simulate prey population vital rates and abundance. We then use simulated data to parameterize and estimate risk for three demographic models (static projection matrix, stochastic projection matrix, stochastic vital rate matrix) and two time series models (diffusion approximation [DA], corrupted diffusion approximation [CDA]). Model bias is measured as the absolute deviation between estimated and observed quasi-extinction risk. Our results highlight three generalities about the application of single-species models to multi-species conservation problems. First, our collective model results suggest that most single-species PVA models overestimate extinction risk when species interactions cause periodic variation in abundance. Second, the DA model produces the most (conservatively) biased risk forecasts. Finally, the CDA model is the most robust PVA to population cycles caused by species interactions. CDA models produce virtually unbiased and relatively precise risk estimates even when populations cycle strongly. High performance of simple time series models like the CDA owes to their ability to effectively partition stochastic and deterministic sources of variation in population abundance.

Key words: corrupted diffusion approximation; extinction; parameter estimation; population cycles; population viability analysis; predator–prey; projection matrix; species interactions; stage structure; stochasticity; time series; vital rate.

Introduction

Demographic rates for single species depend on numerous ecological processes including intrinsic factors (physiological constraints on longevity and fertility) and the effects of environmental variation and other species on these intrinsic factors. While environmental variation is incorporated routinely into demographic studies (Lande 1993, Lande et al. 2003), the effects of species interactions on vital rates of a focal population are not. For example, population models used to manage endangered and/or commercially harvested populations often ignore species interactions (Sinclair et al. 1998, Essington 2004, Sabo 2005). In doing so, one assumes that the vital rates in a life table or a time series of abundance for a single, focal species represent an adequate fingerprint of all of the dynamics embodied in one or many species interactions. In this way, the effects of species interactions are simplified and subsumed by population parameters. Most conservation biologists would agree that this assumption rarely holds in the real world, yet little has been done to quantify the bias introduced when applying a single-species model to a population experiencing strong feedbacks through species interactions. In this paper, we ask: "How wrong are estimates of extinction risk from single-species models that ignore the influence of interactions with other species?"

One potential source of bias introduced by species interactions when implementing PVA is the temporal variation in vital rates and abundance induced by the species interaction itself. For example, predators may cause prey populations to cycle either as a direct result of predation or as an interaction between predation and a variable resource supply for the prey species (Sinclair and Gosline 1997, Stenseth et al. 1998, 1999, Kendall et al. 1999, Turchin et al. 1999, Krebs et al. 2001, Turchin and Hanski 2001, Sinclair et al. 2003). In addition to this deterministic source of variation, environmentally driven variation in predator population abundance can interact with oscillations in prey population abundance (Sabo 2005). Thus, PVA simplifies a dynamic process (the species interaction) into a more static one (constant vital rates or population growth parameters) by assuming that population-level parameters subsume the influences of species interactions. The degree to which a PVA oversimplifies this dynamic process and thereby obscures estimates of extinction risk may in turn depend on the type of PVA model used as well as the quantity and quality of data available when implementing the PVA.

To quantify the bias in risk estimates caused by predator–prey dynamics, we develop a stochastic, stage-structured predator–prey model. This model is first used to generate population data appropriate for five commonly used PVAs (three demographic and two time

Manuscript received 17 April 2006; revised 12 October 2006; accepted 13 October 2006; final version received 25 January 2007. Corresponding Editor: T. E. Essington.

[1] E-mail: John.L.Sabo@asu.edu

series models). These PVA models include (1) diffusion approximation (DA), (2) corrupted DA (CDA), (3) static projection matrix (StaPM), (4) stochastic projection matrix (SPM), and (5) stochastic vital rate matrix (SVR). In all cases, PVA models were parameterized using 15 consecutive years of data (abundance data, projection matrices, or vital rates and their distributions). We then use simulated data to ask which PVA approach gives the most reliable risk estimates for a prey population interacting strongly with a predator. We examine predation because predators are known to cause cycles in prey dynamics—a potential source of bias confounding PVA interpretations. Moreover, introduced predators are a global threat to native prey population viability (Sabo 2005).

The intensity of predation is known to cause nonstructured models of predator–prey interactions to shift between stationary and oscillatory regimes (Beddington et al. 1975, Sabo 2005). In this vein, we ask two more pointed questions about the effect of predator–prey dynamics on PVA risk forecasts: (1) Do predator–prey oscillations bias risk estimates from five commonly applied PVA models in different ways? And, (2) Do these PVA models differentiate between or confound cycles (deterministic variation) and stochastic sources of variation?

Methods

Overview

To understand the biases associated with applying various PVA models to populations experiencing strong species interactions, we employed a split-sample validation approach using simulated data (e.g., Meir and Fagan 2000, Sabo et al. 2004, Gerber et al. 2005). In this paper, this split-sample validation involved three steps (Fig. 1): (1) data generation, (2) parameter estimation, and (3) risk forecasting, and quantification of model bias and precision. Our goal here was to compare the relative bias of five different PVA models in estimating the risk of population declines, or "quasi-extinction" risk. To do this, we first simulated 15 years of data appropriate for each type of PVA. These data consisted of vital rates, projection matrices (emergent properties of vital rates) and time series of abundance for the prey species. Second, we used each type of data to estimate population parameters for a particular PVA model and then simulated population data for 15 additional years using the "estimated" parameters. Finally, we calculated the risk of an 80% decline in abundance using these PVA simulations and compared this "estimated" risk to the real risk. Here real risk was calculated by simulating 15 additional years of population abundance data using the "real" parameters (those used in the first step) but from the same starting abundance used in the PVA simulations. We then calculated the error in each PVA approach as the difference between estimated and real risk. These steps were repeated 1000 times generating a distribution of error in risk estimation. Bias (median error) and precision (dispersion of error) were then used to assess PVA model efficacy. We describe each of these steps in more detail in the following subsections.

Step 1: Simulating structured population data for a predator–prey interaction

We developed a stochastic, stage-structured, predator–prey model based on a similar model (Barbeau and Caswell 1999), but extended by considering explicit feedback between predator and prey species via a prey-dependent predator recruitment function. The model followed the general form

$$\mathbf{N}(t+1) = \mathbf{A}_{\mathrm{N}}^{(t)} \times \mathbf{N}(t) \tag{1a}$$

$$\mathbf{C}(t+1) = \mathbf{A}_{\mathrm{C}}^{(t)} \times \mathbf{C}(t) \tag{1b}$$

where $\mathbf{N}(t)$ and $\mathbf{C}(t)$ are vectors representing the abundance or density of individuals at time t, in each of three stages and $\mathbf{A}_{\mathrm{N}}^{(t)}$ and $\mathbf{A}_{\mathrm{C}}^{(t)}$ are population projection matrices for prey and predators, respectively, in year t [i.e., (t) is not a power function] (see Eqs. 2). In these matrices, we incorporated density dependence in prey fecundity (as $u[N(t)]$), environmental stochasticity in mortality for both species (as $\varepsilon_{\mathrm{N}}^{(t)}$ or $\varepsilon_{\mathrm{C}}^{(t)}$), and a prey-dependent type II functional response (as $v_i[N(t), C(t)]$ or $w_i[N(t), C(t)]$, for prey and predators, respectively), where f_i and F_j are the

$$\mathbf{A}_{\mathrm{N}} = \begin{bmatrix} f_1 \times u[\mathbf{N}(t)] & f_2 \times u[\mathbf{N}(t)] & f_3 \times u[\mathbf{N}(t)] \\ \min\left\{1, \left(1 - v_1[\mathbf{N}(t), \mathbf{C}(t)] + \varepsilon_{\mathrm{N}}^{(t)}\right)\right\} & 0 & 0 \\ 0 & \min\left\{1, \left(1 - v_2[\mathbf{N}(t), \mathbf{C}(t)] + \varepsilon_{\mathrm{N}}^{(t)}\right)\right\} & \min\left\{1, \left(1 - v_3[\mathbf{N}(t), \mathbf{C}(t)] + \varepsilon_{\mathrm{N}}^{(t)}\right)\right\} \end{bmatrix} \tag{2a}$$

$$\mathbf{A}_{\mathrm{C}} = \begin{bmatrix} F_1 \times w_1[\mathbf{N}(t), \mathbf{C}(t)] & F_2 \times w_2[\mathbf{N}(t), \mathbf{C}(t)] & F_3 \times w_3[\mathbf{N}(t), \mathbf{C}(t)] \\ \min\left\{1, \left[1 - \left\{m_1 \times w_1[\mathbf{N}(t), \mathbf{C}(t)] + \varepsilon_{\mathrm{C}}^{(t)}\right\}\right]\right\} & 0 & 0 \\ 0 & \min\left\{1, \left[1 - \left\{m_2 \times w_2[\mathbf{N}(t), \mathbf{C}(t)] + \varepsilon_{\mathrm{C}}^{(t)}\right\}\right]\right\} & S_{\mathrm{C3}} \end{bmatrix} \tag{2b}$$

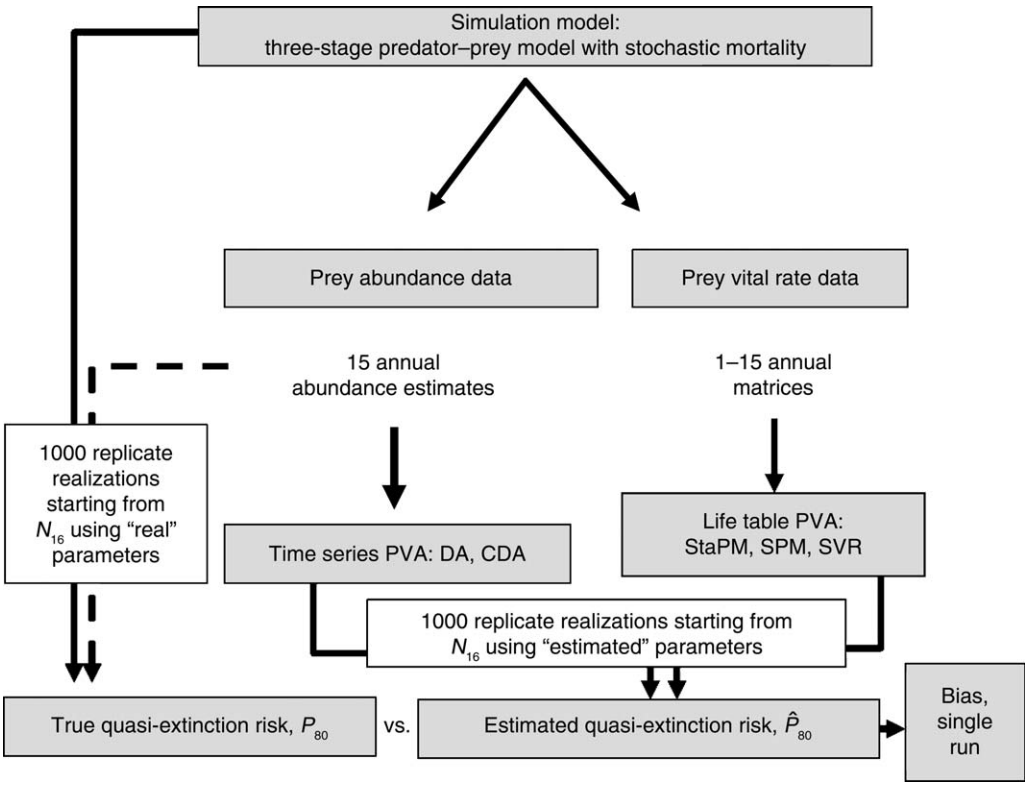

FIG. 1. Schematic showing the methods used to validate five population viability analyses (PVA) models when confronted with data driven by a species interaction. This process is replicated 1000 times for each parameter set of interest. The five PVA models are as follows: the diffusion approximation (DA), the corrupted diffusion approximation (CDA), the static projection matrix model (staPM), the stochastic projection matrix model (SPM), and the stochastic vital rate model (SVR). N_{16} is defined as the first year of the prediction interval, one year after the 15-year fitting interval (hence, N in year 16).

maximum fertilities of the prey of stage i and the predator of stage j, respectively; m_j is the stage-specific, density-independent, mortality rate of the predator; and S_{C3} is the fixed survivorship of the third stage class of the predator. The numerical response of the predator was constrained to its functional response by linking fecundity and stage 1 and 2 survival to the stage-specific encounter and kill rates of prey (via $w_i[\mathbf{N}(t), \mathbf{C}(t)]$). Predator fecundity was further constrained between 0 and F_j. We constrained values for prey (all three stages) and predator (stage 1–2) survival rates, between 0 and 1 (e.g., via $\min\{1, (1 - v_i[\mathbf{N}(t), \mathbf{C}(t)] + \varepsilon_N^{(t)})\}$ and $\min\{1, [1 - (m_j \times w_j[\mathbf{N}(t), \mathbf{C}(t)] + \varepsilon_C^{(t)})]\}$, respectively) to prevent values of this vital rate from exceeding 1 during years when large positive random variates (ε_N or ε_C) were drawn. Finally, low fixed values of stage 3 survival for predators (S_{C3}) resulted in more consistently stable predator–prey interactions.

Implementation of density dependence.—In our model, prey experience density-dependent fertility, with a maximum fertility level (f_i) achieved only at low density and adjusted (downward) as a function of total prey population size. The strength of this density dependence is directly related to the shape parameter, v (Appendix A). In our model, we fixed v at a constant value across all prey stages such that variation in fecundity among age classes (i) varied only with f_i, giving

$$u_i[N(t)] = u[N(t)] = \exp\{-v \times \text{sum}[\mathbf{N}(t)]\}. \quad (3)$$

By contrast, predator fertilities increase to their maximum values (F_j, where j is the age class) as a function of the per capita, stage-specific number of kills, $K_j^{(t)}$ and a scaling constant, γ (Appendix A):

$$w_j[N(t), C(t)] = \exp[-\gamma K_j^{(t)}]. \quad (4)$$

More specifically, we defined $K_j^{(t)}$ as

$$K_j^{(t)} = \sum_{i=1}^{3} \left[\frac{\mu_{i,j} \times N_i^{(t)}}{C_j^{(t)}} \right] \quad (5)$$

where $N_i^{(t)}$ and $C_j^{(t)}$ are stage-specific densities of prey and predator populations at time t, and $\mu_{i,j}$ is the stage-specific mortality rate inflicted by predator stage j on prey stage i.

Implementation of a type II functional response.—Prey were killed and removed from the population as a saturating function of stage-specific density via a type-II functional response where

$$\nu_j[N(t), C(t)] = \mu_{i,j}. \quad (6)$$

We implemented this saturating functional response as Holling's disk equation (Holling 1966:51 [in Barbeau and Caswell 1999:270]). Briefly, the mortality rate experienced by prey class i as a result of predation by predator class j is

$$\mu_{i,j} = \frac{(a_j T_j + b_j) C_j N_i}{1 + \sum_i a_j h_{i,j} \alpha_{i,j} N_i} \tag{7a}$$

where T_j is the total foraging time available for predator class j, $h_{i,j}$ is the handling time of predator class j when handling prey class i, $\alpha_{i,j}$ is the probability of successful capture of prey class i by predator class j (i.e., $P[\text{die} \mid \text{enc}]_{i,j}$ in Barbeau and Caswell 1999). The parameters a_j and b_j relate the body size (radii) and movement velocities of predators and prey to encounter rates of prey:

$$a_j = 2(V_j^2 + U_i^2)^{1/2}(q_j + r_i) \tag{7b}$$

$$b_j = \pi(q_j + r_i)^2 \tag{7c}$$

where V_j and U_i are the movement velocity and q_j and r_i the body size (radius) of the predator and prey species of stage j or i, respectively (see Barbeau and Caswell 1999:271 for more detail). Below we create a range of deterministic variation experienced by prey populations as a result of the predator–prey interaction by altering values of a single parameter, q_j, the predator body radius.

Implementation of environmental stochasticity.—We consider stochasticity in the mortality of predator and prey species. Specifically, stochastic mortality elements ($\varepsilon_{X=\mathrm{N,C}}^{(t)}$) in the model were drawn from a beta distribution (as per Caswell 2000),

$$\varepsilon_{\mathrm{C}}^{(t)}, \varepsilon_{\mathrm{N}}^{(t)} = B(\alpha, \beta) \tag{8}$$

where α and β are transformations of the mean, $\overline{m}_{x=i,j}$, and variance, $\mathrm{var}(m_{x=i,j})$, of the stage-specific (indicated by lowercase x) mortality rates (Morris and Doak 2002):

$$\alpha = \overline{m}_x \times \left[\frac{\overline{m}_x \times (1 - \overline{m}_x)}{\mathrm{var}(m_x)} - 1 \right] \tag{9a}$$

$$\beta = (1 - \overline{m}_x) \times \left[\frac{\overline{m}_x \times (1 - \overline{m}_x)}{\mathrm{var}(m_x)} - 1 \right]. \tag{9b}$$

Step 2: Application of PVA to simulated data

Key features of PVA models examined with simulated data.—There are two broad categories of single-species PVA models—demographic PVA and time series PVA (Morris and Doak 2002). Demographic PVA models include deterministic (hereafter, "static") and two types of stochastic models based on projection matrices (Doak et al. 1994, Heppell et al. 1996, 2000, Mills et al. 1999, Caswell 2000, Wisdom et al. 2000, Morris and Doak 2002). Briefly, these models use empirical estimates of either stage-specific vital rates (i.e., fertility, survival) or projection matrix elements (emergent properties of the vital rates) to calculate the population growth rate (λ_t) and extinction probabilities over a desired time horizon. In static demographic PVA models, vital rates, and thus the projection matrix elements, do not vary in time (as only one projection matrix is used). By contrast, stochastic demographic PVA models incorporate environmental variability in one of two ways—by drawing whole projection matrices at random from a collection of annual, stage-specific, vital rates or by drawing the vital rates from distributions reflecting the means and variances of these rates measured in the field (cf. Morris and Doak 2002: Chapter 8). Below, we refer to these two varieties of stochastic demographic PVA approaches as stochastic projection matrix and stochastic vital rate PVA models, respectively.

Time series PVA models also come in several varieties. The most basic of these is the "diffusion approximation" (hereafter, "DA model" [Lande and Orzack 1988, Dennis et al. 2001]) and the "corrupted DA" model (Holmes 2001, 2004, Holmes and Fagan 2002, Lindley 2003, Staples et al. 2004). Both of these time series models rely on abundance data (15–20 years) to estimate critical growth parameters and forecast risk. The DA model estimates two parameters, the mean (μ) and variance (σ_{p}^2) of annual growth rates, λ_t. The variance in the annual growth rate, σ_{p}^2, is assumed to be driven solely by environmental variation in the environment (i.e., "process error," subscript p). By contrast, the corrupted DA (or CDA) model also estimates the mean, μ, of the annual growth rates but partitions variation due to two sources: process error (σ_{p}^2) and other sources of non-process variation (σ_{np}^2) that include among other things, observation error.

Estimation of population parameters in PVA models.—We parameterized the five PVA models using 15 years of population data for the prey species (vital rates, projection matrices, or abundance data). We chose a 15-year fitting interval as it is the minimum number of abundance estimates required by the most data-hungry time series PVA we analyze: the corrupted diffusion approximation (Holmes 2004). Thus, for each time series, we recorded the total population size, stage-specific population sizes, and the elements of the projection matrix at each time step. In this way, our simulation model provided data amenable to viability analysis by both time series and demographic approaches to PVA. With these data (time series of abundance and projection matrices), we then estimated population growth parameters by applying each PVA model to the same data.

Estimation of parameters for matrix-based, demographic PVAs was straightforward given that our population model yielded the actual data needed for the PVA: annual projection matrices for the prey population (Eq. 2a). These projection matrices (and their elements) were used to estimate $\lambda(t)$ and the means and variances of projection matrix elements (i.e., non-

zero elements in Eq. 2a) from which random projection matrices could be constructed and $\lambda(t)$ values calculated (Morris and Doak 2002). For the static projection matrix model (staPM), we extracted a single projection matrix and used this to calculate $\lambda(t)$. For the stochastic projection matrix model, an entire projection matrix was drawn randomly from the first 15 years of data and used to calculate $\lambda(t)$ at each time step. Finally, in the stochastic vital rate model, we calculated a mean and variance for each element in the projection matrix based on 15 years of data for each element. We then generated unique projection matrices and $\lambda(t)$ values at each time step by drawing random fecundity and survival values from distributions of these elements based on calculated means and variances. Here we assumed a log-normal distribution for variation in fecundity and a beta distribution for variation in survival (following Caswell 2000, Morris and Doak 2002).

The static projection matrix PVA (StaPM) uses only a subset of the total time series (a single projection matrix), and as a result, predictions from these models are highly dependent on "window placement" and the idiosyncrasies of the sequence of the year analyzed (i.e., the sampling window). For example, years of favorable conditions should produce underestimates, and years of unfavorable conditions should produce overestimates of true risk. To control for bias caused by nonrandom window selection of sequential projection matrices, we replicated the parameterization of StaPM model using each of the 15 simulated projection matrices (single projection matrix used for all time steps, 15 total models analyzed). In this way, our implementation of StaPM models mirrors their implementation in the real world, where only a single projection matrix is available, without serendipitously emphasizing idiosyncratic projection matrices.

When using the two time series models (DA and CDA), we estimated population parameters from annual abundance data [e.g., $N(t)$]. The diffusion approximation is a two-parameter model (Lande and Orzack 1988, Dennis et al. 1991)

$$X(t+1) = X(t)\exp(\mu + \varepsilon_t) \qquad \varepsilon_t \sim \text{Norm}(0, \sigma^2_{\text{DA}}) \quad (10)$$

where X is the population size at time t and μ and σ^2_{DA} are parameters describing the average and variance of the annual increase in population size:

$$\lambda(t) = \frac{X(t+1)}{X(t)}.$$

In the simplest case, where data consist of annual censuses with no missing years, μ and σ^2_{DA} can be estimated as the mean and variance of the time series of λ_t

$$\mu = \text{mean}\left\langle \left\{ \ln\left[\frac{X(2)}{X(1)}\right], \ldots \ln\left[\frac{X(t)}{X(t-1)}\right] \right\} \right\rangle \qquad (11a)$$

$$\sigma^2_{\text{DA}} = \text{var}\left\langle \left\{ \ln\left[\frac{X(2)}{X(1)}\right], \ldots \ln\left[\frac{X(t)}{X(t-1)}\right] \right\} \right\rangle \qquad (11b)$$

where $X(t)$ is the prey population size in census year t [i.e., $N(t)$]. We use σ^2_{DA} to denote the process error estimate from the DA model in order to distinguish it from CDA estimates of σ^2_{p} and σ^2_{np}. These estimated parameters can then be used to forecast future population dynamics via Eq. 10. Dennis et al. (1991) give analytic solutions for the probability of population decline to a predetermined threshold level (e.g., probability of 80% decline, or P_{80}) in the last year of a forecasting interval. Analytical solutions for declines (e.g., P_{80}) in any year across the forecasting interval are more cumbersome (Sabo et al. 2004); thus we calculate these declines numerically via Eq. 10 and parameters estimated from independent data using Eq. 11a, b.

The CDA model improves on the simple DA by estimating three parameters, μ, σ^2_{p}, and σ^2_{np}, where σ^2_{p} is process error (i.e., environmental stochasticity) and σ^2_{np} is a second source of error that "corrupts" observations of the true abundance (Holmes 2004). The CDA is a state space model:

$$x(t+1) = x(t) + \mu + \xi(t) \qquad \xi(t) \sim \text{Norm}(0, \sigma^2_{\text{p}}) \quad (12a)$$

$$y(t) = x(t) + \beta + \eta(t) \qquad \eta(t) \sim \text{Norm}(0, \sigma^2_{\text{np}}). \quad (12b)$$

In most applications, this model distinguishes between the true population size, $X(t)$, and the observed population size, $Y(t)$, where $x(t) = \ln[X(t)]$ and $y(t) = \ln[Y(t)]$. True population abundance $[x(t)]$ changes with the mean population growth rate (μ) and random variation $[\xi(t)]$ determined by the variance in the mean growth rate, σ^2_{p}. Observed abundance levels $[y(t)]$ are corrupted by bias (β) and non-process sources of error $[\eta(t)]$. The most common application of state space models is to quantify measurement or "observation" bias and error (Holmes 2004). In this paper, we ignore extrinsic sources of bias and use σ^2_{p} and σ^2_{np} to differentiate between environmental variation and intrinsic variation in prey abundance driven by predator–prey cycles (i.e., $\beta \sim 0$, and $\sigma^2_{\text{np}} \sim$ oscillation amplitude).

There are three general approaches to estimating CDA parameters: a Kalman filter (Lindley 2003), restricted maximum likelihood (ReML) methods (Staples et al. 2004), and the slope method (Holmes 2004). In this paper, we adopted the slope method. Briefly, we first transform "counts" (e.g., $Y(t)$, or $N(t)$ in Eq. 1a, b) into three-year running sums to reduce bias and variability in $\lambda(t)$ due to oscillations arising from non-stable age structure (Holmes 2001, Holmes and Fagan 2002). We then estimate μ as

$$\mu_R = \text{mean}\left\langle \left[\ln\left(\frac{R_2}{R_1}\right), \ldots \ln\left(\frac{R_t}{R_{t-1}}\right) \right] \right\rangle \qquad (13)$$

where $R(t)$ is the running sum transform of $N(t)$. Second, we note that the DA model ignores all non-process error, such that

$$\sigma_{DA} = \sigma_p + \sigma_{np}. \quad (14)$$

One key distinction between process and non-process sources of variation is that the former ($\xi(t)$) feeds back on $x(t)$ and thus, variance in $\lambda(t)$ grows larger with time with σ_p^2. By contrast, $\eta(t)$ does not affect $x(t)$ and thus, $\lambda(t)$ does not grow with σ_{np}^2 over time. Thus, we estimate σ_p^2 as the slope of the variance in $\lambda(t)$ vs. lag (τ) (following Holmes 2001, 2004). Finally, we estimated σ_{np}^2 as the difference between σ_{DA}^2 and σ_p^2 via Eq. 14.

Step 3: Quantifying bias in PVA models via split-sample validation

For the four stochastic PVA models, estimated growth parameters were used to simulate population abundance (1000 replicate realizations) over 15 years (years 16–30). Similarly, we projected 1000 prey populations 15 years into the future (years 16–30) using the "real" parameters (i.e., those used to generate years 1–15) but starting from the same abundance levels as those simulated with the estimated parameters. We calculated probabilities of 80% declines in abundance (P_{80}) for both the "real" population (i.e., the "observed" values from the control, above) and those "estimated" by each PVA model. A quasi-extinction threshold representing an 80% decline in abundance (P_{80}) was chosen based on similar metrics used by the World Conservation Union (IUCN) to classify populations on the Red List of threatened and endangered species (IUCN 2001). Thus we evaluate the ability of each model to predict population size as well as one of the most commonly used risk metrics for endangered species management (see also Sabo et al. 2004, Gerber et al. 2005). Finally, we calculated PVA model bias for each replicate realization as the difference between estimated and observed population decline (i.e., $\hat{P}_{80} - P_{80}$). Thus, positive errors indicate conservative bias, and negative errors indicate overly optimistic risk forecasts (as in Sabo et al. 2004).

Step 4: Implementing two tests of PVA model efficacy

We used the split-sample validation approach described in the preceding section in two complimentary ways. First, we contrasted the bias and precision of PVA models for two parameter sets (Appendix B) representing either stationary deterministic dynamics (no oscillations) or oscillatory dynamics. We hypothesized that PVA models would perform well in spite of predator–prey dynamics as long as predators do not induce cycles (or other deterministic variation) in prey dynamics. To test this hypothesis, we compared bias and precision in $\hat{P}_{80}$ for 1000 replicate realizations among the five PVA models when prey dynamics are either stationary or oscillatory in nature. Second, we quantified the ability of the CDA to differentiate between deterministic and stochastic variation and validate the high performance of this model across a wider range of predator–prey dynamics. Here, we hypothesized that CDA models would generate unbiased and relatively precise estimates of risk ($\hat{P}_{80}$) in spite of predator–prey cycles because CDAs effectively differentiate between deterministic and stochastic variance sources in prey time series of abundance (Holmes 2004). More specifically, we predicted that CDA estimates of σ_{np}^2 should track the deterministic variation associated with predator–prey oscillations and that CDA risk estimates (based on better estimates of σ_p^2) would be both unbiased and relatively precise. We measured the deterministic variation in prey abundance as the "coefficient of intrinsically derived variance": the CV of prey abundance over 1000 years (after a 4000 year burn-in) when $\text{var}(m_{x=i,j}) = 0$.

Starting with the same arbitrary parameter values from our oscillatory parameter set (Appendix B, oscillatory parameter set), we created a gradient of increasing deterministic variation in prey population abundance by increasing values for the body radius of stage-3 predators (q_3) from 1.75 to 3.75. This gradient in deterministic variation was created under two levels of environmental stochasticity ($\text{var}(m_{x=i,j}) = 0.006, 0.012$). With no environmental stochasticity ($\text{var}(m_{x=i,j}) = 0$), changes in q_3 produced a wide range of deterministic model behavior (Fig. 2a), including stable equilibria ($q_3 \sim 1.75$–1.91), chaotic oscillations (e.g., $q_3 \sim 1.95$–2.63) and four- and eight-point limit cycles (e.g., $q_3 \sim 2.75$–3.63). Moreover, the coefficient of variation of prey abundance (i.e., the coefficient of deterministic variation) and the variance in log-transformed annual growth rates of prey populations, i.e.,

$$\text{var}\left[\ln\left(\frac{N_{t+1}}{N_t}\right)\right]$$

increased with q_3 (Fig. 2b, c). The addition of process error increased the variance in ln λ experienced by prey populations but not the relative effect of q_3 on this variation. Values for ln λ increased at a similar rate in deterministic and stochastic model runs and between the two levels of stochasticity examined (compare slopes in Fig. 2c). Values for ln λ produced by our models were similar to the highest values estimated for real populations using density-dependent PVA approaches (e.g., checkerspot butterfly $\sigma_p^2 = 0.65$ [Foley 1994; see Sabo et al. 2004 for summary]). Thus the populations we analyzed represent some of the noisiest realizations one might encounter in the real world, but for our data, we know exactly which components of this noise owe to predators and the environment.

We note here that the relative importance of predator body size in determining the stability of stage-structured predator–prey dynamics in our model (Eq. 2a, b) is beyond the scope of this paper. Instead, we use predator body sizes simply to create a range of deterministic conditions under which a PVA may be administered so that we can better understand the influence of the strength of predator–prey oscillations on the efficacy of PVA. Increasing q_3 leads to increased search efficiency of the predator (via a and b), increased death rates of prey

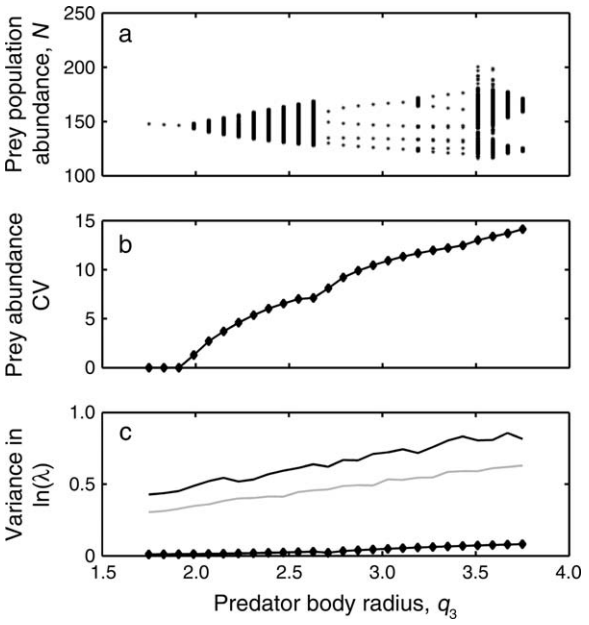

FIG. 2. (a) Bifurcation diagram showing deterministic variation (no process error) in prey abundance (N) as a function of q_3, the body radius of predators in stage class 3. Body size is directly related to the encounter rate between prey and predators in stage class 3. For each value of q_3, we plot 1000 values for total prey population abundance following a 4000-year burn in order to eliminate transient dynamics. (b) Coefficient of deterministically derived variance in prey abundance (no process error) as a function of q_3. (c) Variance in $\ln\lambda$ (i.e., var[$\ln(N_{t-1}/N_t)$]) as a function of deterministic variation brought on by changes in q_3 and three levels of process error ($\sigma_p^2 = 0$, line with solid circles; $\sigma_p^2 = 0.006$, gray line; and $\sigma_p^2 = 0.012$, black line).

(via $\mu_{i,j}$) and increased deterministic variation in prey population dynamics. Increased deterministic variation in turn, sets the stage for understanding key properties of the corrupted diffusion approximation model for PVA.

RESULTS

Single parameter sets: predator–prey oscillations bias some, but not all PVA models

The stationary parameter set led to time series typified by small stochastic variation about a stationary equilibrium for both the prey and predator (Fig. 3a). By contrast, the oscillatory parameter set led to strong and somewhat regular cycles in predator and prey abundance (Fig. 3b). Thus, changes in abundance (and thus vital rates and transition matrices) are relatively constant from year to year under a stationary regime but highly variable under an oscillatory regime.

Quasi-extinction risk was negligible ($P_{80} < 5\%$) for the real population (i.e., the control) under both stationary and oscillatory regimes. All five models predict this precisely and accurately under a stationary regime (Fig. 4a). By contrast, all PVA models except the corrupted DA overestimate extinction risk as measured by P_{80} when prey populations cycle as a result of strong predation (oscillatory regime, Fig. 4b). The DA model overestimates risk by as much as 40%. Static demographic PVA models produce risk estimates that are either 100% or 0% (i.e., inter-quartile range of 0–1), depending on the year in which the projection matrix is extracted from the original time series. On average, bias (i.e., median error) is much lower and still conservative, for the stochastic demographic PVA models (vital rate or projection matrix). However, these models give highly imprecise estimates of risk, some giving errors as high as 90%. Moreover, demographic PVAs are more likely to underestimate P_{80}, than time series models given the same data. In summary, only the corrupted DA model accurately (and precisely) estimated P_{80} for both stationary and cycling populations interacting with a predator. Below we explore the generality of low bias and high precision of the CDA model across a wider range of predator–prey dynamic behavior.

CDA performance when confronted with deterministic and stochastic sources of variation

An increase in the body radius of stage-3 predators (q_3) led to increases in prey death rates and concomitant increases in deterministically driven variation in prey population dynamics (Fig. 2b). Environmental stochasticity [via var($m_{x=i,j}$)] further increases variation in prey abundance (Fig. 2c). Time series for most of this parameter space are noisy (Fig. 5), some remaining

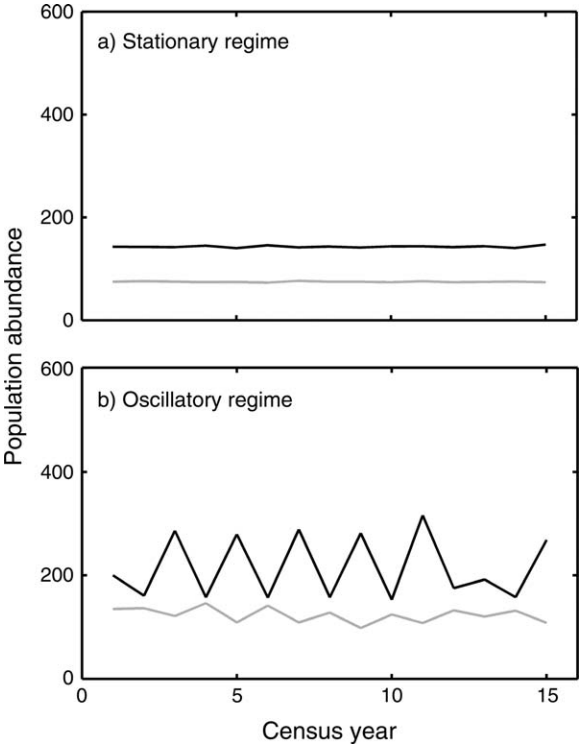

FIG. 3. Population trajectories for prey (black line) and predator (gray line) populations generated by single representative (a) stationary and (b) oscillatory parameter sets (see Appendix B).

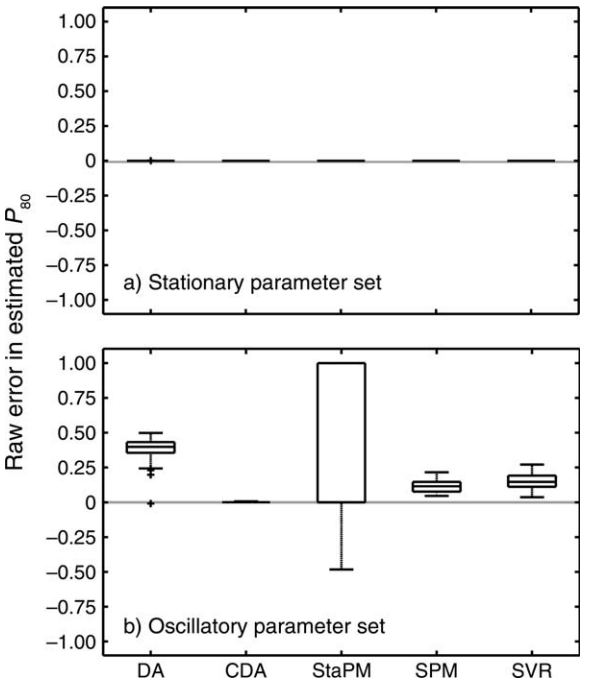

FIG. 4. Raw error in the estimation of the probability of an 80% decline (P_{80}) for each of five commonly used population viability analyses (PVA) models under the (a) stationary and (b) oscillatory parameter sets. PVA models are the diffusion approximation (DA), the corrupted DA (CDA), static projection matrix PVA (StaPM), and stochastic demographic PVAs based on projection matrices (SPM) or vital rates (SVR). Boxes are medians (middle line) and upper and lower quartiles, whiskers are 1.5× the range contained by the upper and lower quartiles, and crosses indicate outliers. Positive and negative errors indicate over- and underestimation of P_{80}, respectively.

close to a stationary equilibrium (i.e., where q_3 is low) and others varying more widely, and crossing our quasi-extinction threshold more readily [i.e., high q_3 and high var($m_{x=i,j}$)]. In all cases, variation is high and in part driven by deterministic in addition to stochastic sources of variation. True quasi-extinction risk (P_{80}) is correspondingly much higher than in our previous analysis, ranging from 0 to 99%. Here we evaluate how well the CDA model attributes deterministic and stochastic sources of variation to non-process (σ^2_{np}) and process error (σ^2_p) components of the model. If the CDA effectively attributes deterministic variation to σ^2_{np}, this would explain the high accuracy and precision of risk forecasts made by this model in spite of predator induced variation in prey abundance.

CDA estimates of σ^2_{np} increased with the coefficient of intrinsically derived variance (Fig. 6). This result was nearly identical at both levels of process error added to prey and predator vital rates [var($m_{x=i,j}$)]. In both cases, $\hat{\sigma}^2_{np}$ are high even when intrinsic variation is near zero. We hypothesize that the CDA model attributes both deterministic variation and variation caused by the interaction between stochastic and deterministic sources of variation to σ^2_{np}. For example, environmental stochasticity (via var($m_{x=i,j}$)) may prolong otherwise transient oscillations in prey abundance, and these oscillations are interpreted by CDA models as σ^2_{np}, rather than a third source of variance associated with the interaction between σ^2_p and σ^2_{np}. In contrast to a relatively steep increase in $\hat{\sigma}^2_{np}$ with the coefficient of intrinsically derived variance, estimated levels of process error in prey abundance (σ^2_p) were more nearly identical across this range of deterministic variation in prey abundance, reflecting the constant source of environmental variation added to prey and predator vital rates via var($m_{x=i,j}$).

As a result of effective partitioning of deterministic and stochastic sources of variation (Fig. 6), CDA estimates of quasi-extinction risk ($\hat{P}_{80}$) were nearly unbiased across a 25% increase in intrinsically driven variation in prey abundance (Fig. 7) and at both levels of environmental stochasticity added to prey and predator vital rates. Surprisingly, the inter-quartile range of CDA quasi-extinction estimates was small

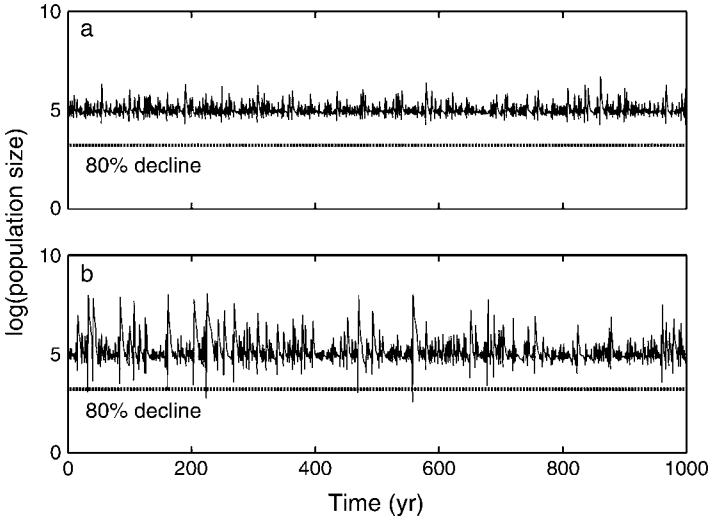

FIG. 5. Representative time series of abundance for prey populations (N_t). (a) Low stochastic variation [var($m_{x=i,j}$) = 0.006; see Eq. 9a, b] and low deterministic variation (predator body size in stage 3, $q_3 = 1.75$). (b) High relative stochastic variation [var($m_{x=i,j}$) = 0.012] and high deterministic variation ($q_3 = 3.75$). In both panels, we plot the prey population level corresponding to an 80% decline from N_1 (the abundance in year 1). Prey populations were more likely to reach this quasi-extinction threshold when stochastic and deterministic variation were simultaneously high.

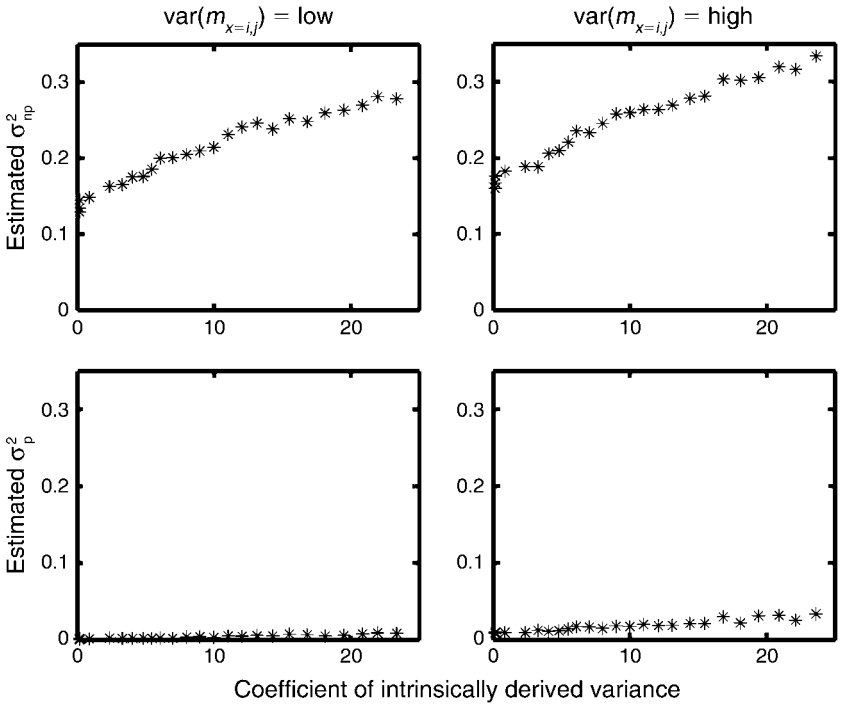

FIG. 6. Corrupted diffusion approximation model estimates for non-process error (σ^2_{np}, top panels) and process error (σ^2_{p}, bottom panels) as a function of the coefficient of intrinsically derived variance in prey abundance (brought on by changes in q_3 [predator body size in stage 3]). The coefficient of intrinsically derived variance is the CV of 1000 prey population sizes for each value of q_3 in Fig. 4. Panels show mean estimates for 1000 replicate realizations (of prey populations) with a given value for q_3 and either low environmental stochasticity [left-hand panels, var($m_{x=i,j}$) = 0.006; see Eq. 9a, b] or high environmental stochasticity [right-hand panels, var($m_{x=i,j}$) = 0.012].

suggesting relatively high precision of CDA risk forecasts as well (Fig. 7).

DISCUSSION

Single-species PVA models assume that the dynamic effects of one, or many, species interactions experienced by the focal species are subsumed by fecundity, survival, or population abundance. Our analyses illustrate how this practice may oversimplify community level phenomena and bias population forecasts made by some, but not all, PVA models. Specifically, our results highlight three observations about the perils associated with blind application of single-species models to prey populations whose dynamics are strongly influenced by predation.

First, most single-species PVA models overestimate extinction risk (e.g., conservative estimation) when species interactions cause periodic variation or cycles in abundance (Figs. 2 and 4b). This result is consistent with other simulation studies that have examined how cycling (Sabo et al. 2004) or periodic (rather than

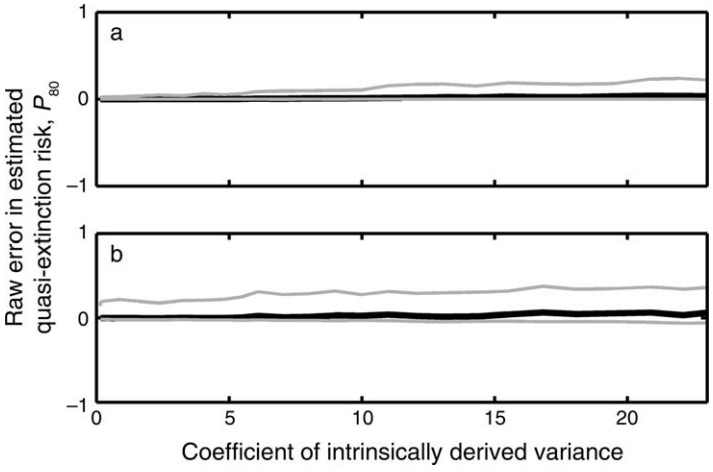

FIG. 7. Median (thick black line) and 25th and 75th percentile (thin gray lines) values for bias in estimates of 80% declines (bias = $\hat{P}_{80} - P_{80}$) as a function of deterministic variation in prey abundance related to the size of predators in stage 3 (q_3). Panels show results for simulations with (a) low and (b) high environmental stochasticity in the survival of predator and prey species [i.e., var($m_{x=i,j}$); see Eqs. 9a, b].

stochastic) variation in abundance of a single species can in many cases result in strong overestimation of risk (K. Buenau, J. L. Sabo, and L. R. Gerber, *unpublished manuscript*). Thus, bias in single-species models will tend to err in favor of conservation, predicting more dire risk than the target population is likely to experience over the prediction interval. This conservative bias could have positive and negative consequences for conservation efforts. Conservative risk estimates may guarantee the protection of the target species over a wider range of conditions; however, erroneous risk estimates may decrease public confidence in conservation science and increase conflict between the governmental agencies responsible for the management of target species and public stakeholders. The low bias in CDA risk estimates suggests that some single-species models will provide relatively accurate risk forecasts even when confronted with strongly oscillatory data.

Second, not all single-species PVA models are equal when confronted with a focal population that exhibits cycles as a result of predation. Static demographic PVAs give gross over- and underestimates of risk depending on the period in which the parameters are estimated. Risk estimates will be overly optimistic when model parameters are estimated across years of increasing abundance; conversely, risk will be overestimated when parameters are estimated during bust years. Bias is lower and conservative, and precision is higher for the stochastic vital rate model. Nevertheless, bias was still significantly higher for this model than for the CDA.

Third, only the corrupted DA model is able to adequately differentiate between environmentally driven variation in mean growth rates, and variation driven by predator-induced cycling. Thus, the corrupted DA model most consistently produced accurate risk forecasts for the specific stationary or oscillatory parameter sets examined here. Moreover, CDA risk estimates are unbiased and relatively precise across a wide range of parameter space that includes both high and low deterministic and stochastic variation in prey abundance.

Why does the CDA work so well?

Corrupted diffusion models are designed to differentiate between process and a non-process source of error: typically observation error or oscillations related to departures from stable-age structure. Process error results from variation in the environment (environmental stochasticity) and can be detected as an increase in the variance in $\ln[N(t+\tau)/N(t)]$ with τ, where τ is the lag in years between abundance estimates. For example, the variance in the log ratio of abundance estimates eight years apart may be higher than the variance between abundance estimates two years apart. Non-process sources of error affect both the numerator and denominator of $\ln[N(t+\tau)/N(t)]$ independently of τ. The variance of $\ln[N(t+\tau)/N(t)]$ with process and non-process error is then (for τ not too large) $\tau\sigma_p^2 + 2\sigma_{np}^2$. Thus, the slope and half of the value of the intercept of the relationship between lag (τ, or years between abundance estimates) and variance in $\ln[N(t+\tau)/N(t)]$ give estimates of process and observation error, respectively (cf. Holmes 2004: Eq. 14). We demonstrate that CDA viability models differentiated between predator–prey cycles and environmental stochasticity. As such, CDAs produced unbiased quasi-extinction estimates even when predators caused strong variation in prey abundance. CDA models filtered cycles (as σ_{np}^2) and estimated risk with a more appropriate estimate of stochastic variation (σ_{np}^2).

Generality of predator–prey dynamics analyzed

Our predator–prey model (Eq. 2a, b) is complex but similar in nature to unstructured deterministic models used commonly in food web science (e.g., Murdoch and Oaten 1975, Oksanen et al. 1981, Moore et al. 2004). For example, the model has prey density dependence and a type II functional response derived from Holling's classic disk equation (Holling 1959). The model also couples predator fecundity and survival directly to prey consumption. Finally, we add stochasticity to prey and predator survival rates in a traditional way (Caswell 2000). The behavior that the model generates is quite broad, ranging from stationary, but stochastic fluctuations around equilibrium abundance levels, to limit cycles and chaos (Fig. 2a). Our results suggest that not all PVA models are equal when confronted with prey dynamics that are both oscillatory and stochastic. Predator-induced oscillations bias estimates of process error in all PVA models accept the CDA. Moreover, significant shifts in the qualitative behavior of prey dynamics produce negligible bias and only moderate imprecision in CDA estimates of P_{80} (Fig. 7). Thus, while our analysis makes the direct comparison of all 5 PVA models for only a subset of predator–prey behaviors (i.e., stationary and oscillatory), our evaluation of the performance of the CDA model considers a much broader range of conditions (i.e., true extinction risk). CDA estimates of risk remain robust despite strong cycles and chaos in prey dynamics mediated by predation.

Caveats

Our conclusions are limited in scope by at least three simplifications in our analyses. First, we compared the performance of all five PVA models under only two sets of prey dynamics and in both cases the true risk of prey population decline (P_{80}) is low ($\sim$0% and $<$2% for the stationary and oscillatory parameter sets, respectively). The relative performance of these five models may differ when this risk is much higher. In our more extensive analysis of the CDA model, we observed negligible bias across a wider range of true risks of decline ($P_{80} \sim$ 0–99%). Thus, our results represent a starting point for assessing the efficacy of PVA when confronted with population data drive by predator–prey dynamics. Specifically, when true quasi-extinction risk is low, most PVAs will grossly overestimate risk while the CDA will provide more accurate and relatively precise estimates of

P_{80}. High accuracy and precision of the CDA is robust across a wide range of "true" risk.

Second, our analyses ignore the potentially confounding effects of observation error as an additional source of non-process variation. Of the PVA models examined here, only two (the corrupted DA and stochastic vital rate models) are capable of differentiating between observation and process error. In this study, we found that the corrupted DA was also capable of distinguishing between environmental sources of variation (i.e., σ_p^2) and predator induced variation (as σ_{np}^2). Thus, the efficacy of the corrupted DA may differ when prey time series are corrupted by both predator–prey cycles and observation error. It is likely that the inclusion of observation error in our simulation models would favor PVA models that require fewer data. Fewer bad data used to parameterize the PVA produce fewer errors in forecasting risk. Thus, the four models rank in the following order in terms of the required number of field estimates (assuming three age or stage classes as in Eq. 2a, b): static demographic model (six vital rates), DA model (10 abundance estimates, minimum), the corrupted DA model (15 abundance estimates, minimum), and the stochastic demographic model (18 vital rates, minimum). This suggests that the large differences in efficacy of the four models observed in this study may be diminished when one considers the amount of (potentially bad) data required for each. Future studies should investigate the effects of trade-offs between data requirements (number of years or vital rates), the relative magnitude of observation error associated with field estimates of vital rates and abundance data, and the costs of collecting either type of data.

Third, our analysis includes interactions between only two species and does not evaluate the effect of other types of species interactions (e.g., competition, mutualism). The net effects (direct and indirect) of interactions with the full diversity of species comprising the community may either augment or diminish the bias in risk estimation brought on by one strongly interacting species. Improvements in the statistical approaches to analyzing community persistence (Ives et al. 2003) place us in a position to address questions about the effects of diversity on the persistence of single species within larger communities.

Conclusion

Population models, including PVA, necessarily simplify the complexity of species interactions (Murdoch et al 2002, Sabo et al. 2005). This complexity is implicitly subsumed by vital rates in a population model. Our results suggest that this practice can be misleading, but only when the single-species model is itself overly complex. Vital rates in a six parameter, stage-structured matrix model do not accurately characterize the dynamic nature of predator–prey cycles. Surprisingly, a much simpler (three parameter) statistical description of the population trend (the CDA model) outperforms more complex matrix models at characterizing future population dynamics as indexed by the risk of quasi-extinction (P_{80}). Both models assume the wrong process of population growth, yet the simpler of these wrong models is more effective at forecasting extinction metrics.

This result lends support to a growing body of theory advocating simple models to describe complex processes. For example, Murdoch et al. (2002) demonstrate that the cycle period for an interaction between a generalist predator and prey population converges on the range of periods expected by a single population process. Here, a simple statistical description of a single-species population dynamic (e.g., scaled cycle period) suffices despite the complications of a predator–prey interaction. In a similar vein, fisheries models that are fitted to time series data (e.g., "inverse" models) often provide better predictions of optimal effort than "process" based food web models that incorporate more complex species interactions (Essington 2004). Inverse models describe trends in data better than process models even if they are no more biologically correct than process models.

In this paper, a simple inverse model (the CDA) outperforms more complex process models of single-species population dynamics (e.g., matrix models) at forecasting extinction risk. The strength of the simple model hinges on a trade-off between biological plausibility and descriptive accuracy. CDA models more accurately describe stochastic and deterministic sources of variation inherent in a short time series than more plausible matrix models and this descriptive advantage leads them to more accurate portrayals of extinction risk.

Acknowledgments

We thank Peter Abrams, Steve Beissinger, Mike Booth, Barry Brook, Beth Hagen, Tammy Harms, Andy Keller, Kevin McCluney, Hugh Possingham, Candan Soykan, Lewi Stone, and seven anonymous reviewers for comments on previous versions of this paper. We also thank Eli Holmes for code and guidance with the corrupted diffusion approximation and discussions about diffusion approximations and the application of statistical models to data.

Literature Cited

Barbeau, M. A., and H. Caswell. 1999. A matrix model for short-term dynamics of seeded populations of sea scallops. Ecological Applications 9:266–287.

Beddington, J. R., C. A. Free, and J. H. Lawton. 1975. Dynamic complexity in predator–prey models framed in difference equations. Nature 255:58–60.

Caswell, H. 2000. Matrix population models: construction, analysis, and interpretation. Second edition. Sinauer, Sunderland, Massachusetts, USA.

Dennis, B., R. A. Desharnais, J. M. Cushing, S. M. Henson, and R. F. Costantino. 2001. Estimating chaos and complex dynamics in an insect population. Ecological Monographs 71:277–303.

Doak, D., P. Kareiva, and B. Kleptetka. 1994. Modeling population viability for the desert tortoise in the western Mojave Desert. Ecological Applications 4:446–460.

Essington, T. E. 2004. Getting the right answer from the wrong model: evaluating the sensitivity of multispecies fisheries advice to uncertain species interactions. Bulletin of Marine Science 74:563–581.

Foley, P. 1994. Prediciting extinction times from environmental stochasticity and carrying capacity. Conservation Biology 8: 124–137.

Gerber, L. R., H. McCallum, K. D. Lafferty, J. L. Sabo, and A. Dobson. 2005. Exposing extinction risk analysis to pathogens: Is disease just another form of density dependence? Ecological Applications 15:1402–1414.

Heppell, S. S., H. Caswell, and L. B. Crowder. 2000. Life histories and elasticity patterns: perturbation analysis for species with minimal demographic data. Ecology 81:654–665.

Heppell, S. S., L. B. Crowder, and D. T. Crouse. 1996. Models to evaluate headstarting as a management tool for long-lived turtles. Ecological Applications 6:556–565.

Holling, C. S. 1959. The components of predation as revealed by a study of small-mammal predation of the European pine sawfly. Canadian Entomologist 91:293–320.

Holmes, E. E. 2001. Estimating risks in declining populations with poor data. Proceedings of the National Academy of Sciences (USA) 98:5072–5077.

Holmes, E. E. 2004. Beyond theory to application and evaluation: diffusion approximations for population viability analysis. Ecological Applications 14:1272–1293.

Holmes, E. E., and W. E. Fagan. 2002. Validating population viability analysis for corrupted data sets. Ecology 83:2379–2386.

IUCN. 2001. IUCN Red List categories and criteria. Version 3.1. IUCN Species Survival Commission. IUCN, Gland, Switzerland and Cambridge, UK.

Ives, A. R., B. Dennis, K. L. Cottingham, and S. R. Carpenter. 2003. Estimating community stability and ecological interactions from time-series data. Ecological Monographs 73: 301–330.

Kendall, B. E., C. J. Briggs, W. W. Murdoch, P. Turchin, S. P. Ellner, E. McCauley, R. M. Nisbet, and S. N. Wood. 1999. Why do populations cycle? A synthesis of statistical and mechanistic modeling approaches. Ecology 80:1789–1805.

Krebs, C. J., R. Boonstra, S. Boutin, and A. R. E. Sinclair. 2001. What drives the 10-year cycle of snowshoe haves? BioScience 51:25–35.

Lande, R. 1993. Risks of population extinction from demographic and environmental stochasticity and random catastrophes. American Naturalist 142:911–927.

Lande, R., S. Engen, and B.-E. Sæther. 2003. Stochastic population dynamics in ecology and conservation. Oxford University Press, Oxford, UK.

Lande, R., and S. H. Orzack. 1988. Extinction dynamics of age-structured populations in a fluctuating environment. Proceedings of the National Academy of Sciences (USA) 85: 7418–7421.

Lindley, S. T. 2003. Estimation of population growth and extinction parameters from noisy data. Ecological Applications 13:806–813.

Meir, E., and W. F. Fagan. 2000. Will observation error and biases ruin the use of simple extinction models? Conservation Biology 14:148–154.

Mills, L. S., D. F. Doak, and M. J. Wisdom. 1999. Reliability of conservation actions based on elasticity analysis of matrix models. Conservation Biology 13:815–829.

Moore, J. C., et al. 2004. Detritus, food web dynamics and biodiversity. Ecology Letters 7(7):584–600.

Morris, W. F., and D. F. Doak. 2002. Quantitative conservation biology: theory and practice of population biology. Sinauer and Associates, Sunderland, Massachusetts, USA.

Murdoch, W. W., B. E. Kendall, R. M. Nisbet, C. J. Briggs, E. McCauley, and R. Bolser. 2002. Single-species models for many-species food webs. Nature 417:541–543.

Murdoch, W. W., and A. Oaten. 1975. Predation and population stability. Advances in Ecological Research 9:1–131.

Oksanen, L., S. D. Fretwell, J. Arruda, and P. Neimela. 1981. Exploitation ecosystems in gradients of primary productivity. American Naturalist 118:240–261.

Sabo, J. L. 2005. Stochasticity, predator–prey dynamics and trigger harvest of nonnative predators. Ecology 86:2329–2343.

Sabo, J. L., B. E. Beisner, E. L. Berlow, K. Cuddington, A. Hastings, M. Koen-Alonso, G. D. Kokkoris, K. McCann, C. J. Melián, and J. C. Moore. 2005. Population dynamics and food web structure: predicting measurable food web properties with minimal detail and resolution. Pages 437–450 *in* P. de Ruiter, V. Wolters, and J. C. Moore, editors. Dynamic food webs: multispecies assemblages, ecosystem development, and environmental change. Elsevier, London, UK.

Sabo, J. L., E. E. Holmes, and P. Kareiva. 2004. Efficacy of simple viability models in ecological risk assessment: Does density dependence matter? Ecology 85:328–341.

Sinclair, A. R. E., D. Chitty, C. I. Stefan, and C. J. Krebs. 2003. Mammal population cycles: evidence for intrinsic differences during snowshoe hare cycles. Canadian Journal of Zoology–Revue Canadienne De Zoologie 81:216–220.

Sinclair, A. R. E., and J. M. Gosline. 1997. Solar activity and mammal cycles in the northern hemisphere. American Naturalist 149:776–784.

Sinclair, A. R. E., R. P. Pech, C. R. Dickman, D. Hik, P. Mahon, and A. E. Newsome. 1998. Predicting effects of predation on conservation of endangered prey. Conservation Biology 12:564–575.

Staples, D. F., M. L. Taper, and B. Dennis. 2004. Estimating population trend and process variation for PVA in the presence of sampling error. Ecology 85:923–929.

Stenseth, N. C., et al. 1999. Common dynamic structure of Canada lynx populations within three climatic regions. Science 285:1071–1073.

Stenseth, N. C., W. Falck, K. S. Chan, O. N. Bjornstad, M. O'Donoghue, R. Tong, R. Boonstra, S. Boutin, C. J. Krebs, and N. G. Yoccoz. 1998. From patterns to processes: phase and density dependencies in the Canadian lynx cycle. Proceedings of the National Academy of Sciences (USA) 95:15430–15435.

Turchin, P., and I. Hanski. 2001. Contrasting alternative hypotheses about rodent cycles by translating them into parameterized models. Ecology Letters 4:267–276.

Turchin, P., A. D. Taylor, and J. D. Reeve. 1999. Dynamical role of predators in population cycles of a forest insect: an experimental test. Science 285:1068–1071.

Wisdom, M. J., L. S. Mills, and D. F. Doak. 2000. Life stage simulation analysis: estimating vital-rate effects on population growth for conservation. Ecology 81:628–641.

APPENDIX A

Detailed descriptions of stochastic stage-structured predator–prey model (*Ecological Archives* A017-061-A1).

APPENDIX B

Parameter values for stable and oscillatory regimes (*Ecological Archives* A017-061-A2).